Ecosystems (2018) 21: 1348–1363
https://doi.org/10.1007/s10021-018-0225-5

Change in Vegetation Patterns Over a Large Forested Landscape Based on Historical and Contemporary Aerial Photography

Jamie M. Lydersen[1,2]* and Brandon M. Collins[3]

[1]*USDA Forest Service, Pacific Southwest Research Station, 1731 Research Park Dr, Davis, California 95618, USA;* [2]*Department of Environmental Science, Policy and Management, University of California, Berkeley, Berkeley, California, USA;* [3]*Center for Fire Research and Outreach, University of California, Berkeley, 137 Mulford Hall, Berkeley, California 94720, USA*

Abstract

Changes to vegetation structure and composition in forests adapted to frequent fire have been well documented. However, little is known about changes to the spatial characteristics of vegetation in these forests. Specifically, patch sizes and detailed information linking vegetation type to specific locations and growing conditions on the landscape are lacking. We used historical and recent aerial imagery to characterize historical vegetation patterns and assess contemporary change from those patterns. We created an orthorectified mosaic of aerial photographs from 1941 covering approximately 100,000 ha in the northern Sierra Nevada. The historical imagery, along with contemporary aerial imagery from 2005, was segmented into homogenous vegetation patches and classified into four relative cover classes using random forests analysis. A generalized linear mixed model was used to compare topographic associations of dense forest cover on the historical and contemporary landscapes. The amount of dense forest cover increased from 30 to 43% from 1941 to 2005, replacing moderate forest cover as the most dominant class. Concurrent with the increase in extent, the area-weighted mean patch size of dense forest cover increased tenfold, indicating greater continuity of dense forest cover and more homogenous vegetation patterns across the contemporary landscape. Historically, dense forest cover was rare on southwesterly aspects, but in the contemporary forest, it was common across a broad range of aspects. Despite the challenges of processing historical air photographs, the unique information they provide on landscape vegetation patterns makes them a valuable source of reference information for forests impacted by past management practices.

Key words: image object analysis; historical aerial photography; landscape restoration; vegetation change; landscape vegetation pattern; Sierra Nevada.

Received 14 June 2017; accepted 11 January 2018; published online 5 February 2018

Electronic supplementary material: The online version of this article (https://doi.org/10.1007/s10021-018-0225-5) contains supplementary material, which is available to authorized users.

Author Contributions JL designed the study, performed research, analyzed data, and wrote the paper. BC conceived and designed the study and wrote the paper.

**Corresponding author; e-mail:* jmlydersen@fs.fed.us

Introduction

Management of forested landscapes in the Western USA is often focused on reversing vegetation change that occurred following decades of fire exclusion and timber harvest focused on large tree removal (North and others 2009; Fulé and others

2012; Larson and others 2012; Lydersen and others 2017). Landscape-level vegetation patterns are gaining increased attention due to greater understanding of their influence on ecosystem processes such as wildfire, hydrology, and wildlife diversity (Hessburg and others 2000; Collins and others 2007; Boisramé and others 2016; Tingley and others 2016). Historical forest conditions provide critical insight into understanding how intact disturbance regimes interacted with topographic and edaphic settings to shape vegetation patterns across landscapes. These historical conditions are also used to assess departure in contemporary forests from the natural range of variability (Moore and others 1999; Churchill and others 2013; Hagmann and others 2013, 2014; Barth and others 2015; Collins and others 2015; Stephens and others 2015; Clyatt and others 2016). Data on historical forest conditions, in the form of both reconstructions and archived records, can provide detailed information for ranges of tree density, basal area, and species composition over large areas (> 10,000 ha), but they are limited in the amount of inference that can be made about landscape vegetation patterns because they lack comprehensive spatial coverage. Specifically, many historical reconstructions are missing important landscape-level spatial characteristics such as vegetation patch sizes and detailed information linking vegetation type to specific locations and growing conditions on the landscape (Dickinson 2014; Collins and others 2015).

Aerial photography provides an additional source of information on historical vegetation patterns. Historical aerial photographs are widely available in many locations, but they are underutilized due to constraints such as the cost and time required for processing (Morgan and others 2010; Morgan and Gergel 2013). Automated approaches to classifying vegetation in historical imagery are becoming more widely available (Eitzel and others 2016), leading to increased interest in using aerial photography to assess vegetation change and historical landscape patterns. Historical aerial photographs offer several advantages over other forms of historical or reference vegetation data. When processed into a continuous, orthorectified photograph mosaic, they comprehensively cover a large area and provide information relevant to large-scale disturbances such as wildfire and insect outbreaks, as well as habitat for wildlife species with large home ranges. While traditional plot-based field data are limited to specific locations and within-patch vegetation descriptions, photograph mosaics provide detailed information on vegetation patch sizes and extent (Airey Lauvaux and others 2016). Historical photograph mosaics also provide spatially explicit data across a range of vegetation conditions (for example, montane chaparral, meadow), whereas many reconstructions tend to be focused on tree-dominated portions of landscapes. Having complete coverage over an entire area avoids both bias in sampling location and the need to assume plot locations are representative of the nearby area.

The extent and configuration of dense forest (for example, > 60% canopy cover) are of particular interest due to their conflicting attributes of providing habitat for wildlife species of concern while being prone to stand-replacing fire (Jones and others 2016). Historical timber survey data collected over large areas suggest that forests adapted to frequent fire (for example, mean fire return interval of 11–16 years; Van de Water and Safford 2011) were very open historically, on average (10–30% canopy cover) (Collins and others 2015; Stephens and others 2015; Hagmann and others 2017). This is difficult to reconcile with the contemporary habitat requirements of some species, such as moderate-to-large patches (> 100 ha) of dense tree canopy cover for nesting and roosting (Tempel and others 2015). Large patches of dense forests are vulnerable to stand-replacing fire, and at current rates of burning, their persistence into the future is uncertain (Stephens and others 2016). In addition, these patches may be more susceptible to drought-related tree mortality (Bradford and Bell 2017; Young and others 2017). One explanation for how forests that were generally open also provided habitat for dense forest associates is that historical landscapes had much greater heterogeneity. There is some evidence indicating that historical forest landscapes included openings and areas of low canopy density interspersed with patches of denser tree cover (Hessburg and others 2007; Brown and others 2008). It has been hypothesized that this configuration allowed for greater overall resilience by limiting tree crown and patch connectivity across the landscape (Hessburg and others 2005; Kennedy and Wimberly 2009; Hessburg and others 2015).

It is generally accepted that historical forests had patchy spatial structure (Show and Kotok, 1924; Sánchez Meador and others 2009). However, the specific processes that drove this patchiness are not well known. Current restoration guidelines suggest that patches of dense forest be aligned with topography, with denser forest patches being retained on north facing slopes and in canyon bottoms (North and others 2009). This advice has been based on contemporary reference information (for example, Lydersen and North 2012) and reconstructions of historical forest structure (Beaty and Taylor 2001, 2008). However, reconstructions in some areas suggest that under an intact disturbance regime variation in forest structure was not strongly associated with topographic or productivity gradients, but the influence of these gradients became more pronounced following fire exclusion (Abella and others 2015; Johnston and others 2016). Clearly, more information is needed on the historical extent and drivers of dense forest across frequent-fire landscapes.

In this study, we used historical aerial photographs across a large landscape (100,000 ha) to characterize historical vegetation patterns and assess contemporary change from those patterns. Our goal was to use this spatially comprehensive information to fill gaps in the current knowledge on variability in historical versus contemporary landscapes. The historical photographs were taken in 1941. Although 1941 certainly does not capture an unperturbed forest condition, it does predate heavily mechanized fire suppression and timber harvesting in our study area. Our objectives were to (1) quantify patch size and extent of vegetation types, (2) determine the extent to which topographic factors are associated with the distribution of dense forest cover, and (3) compare the patterns of dense forest cover observed in 1941 to contemporary vegetation patterns.

Methods

Study Area

The study area is located in Plumas National Forest in the northern Sierra Nevada (Figure 1A). The area for which historical and contemporary images was obtained is approximately 150,000 ha in size, but we limited our analysis to Forest Service land, which totaled 100,526 ha (Figure 1B). Contemporary dominant vegetation alliances within the analysis area include mixed conifer—Fir (30%), Douglas-fir—pine (19%), eastside pine (15%), mixed conifer—pine (12%), and Big Sagebrush (5%) (Forest Service Region 5 2000–2014 Existing Vegetation data). Forests in the area are associated with a historically frequent, mainly low-severity fire regime (Moody and others 2006). Burning was relatively uncommon from 1941 to 2005 with recorded fires affecting 12% of the total analysis area (The California Department of Forestry and Fire Protection's Fire and Resource Assessment Program). Fires documented prior to 1941 were more uncommon, affecting 6% of the total analysis area (Figure 1C). Archived records with the Heritage Resources staff indicated that widespread timber harvesting had not occurred in this area prior to 1941 (pers. comm., D. Elliot, Plumas National Forest 2016). This is corroborated by the lack of an extensive road network in the 1941 aerial photographs.

1941 Image Processing

Black and white aerial photographs taken in 1941 over portions of Lassen, Plumas, Shasta, and Tehama counties at a photoscale of 1:20,000 were processed and used for vegetation analysis (Figure 2). Aerial photonegatives for 238 photographs covering the 150,000 ha study area were digitized by a private contractor at a resolution of 600 dots per inch. Along with the photographs, we obtained a copy of a hand drawn map from 1941 showing the approximate locations of the photographs across Plumas National Forest. Photographs within our study area were collected between 30 September and 10 November 1941. Photographs were collected midday, ranging from 10:55 to 14:10, when shadowing was less apparent.

An orthorectified photograph mosaic was generated using Historical Airphoto Processing version 2.1 and Geomatica 2014 (PCI Geomatics 2015, 2014). Orthorectification improves the horizontal accuracy of aerial imagery by adjusting for image perspective and terrain distortions so that each pixel appears as it would if collected from directly overhead. National Agriculture Imagery Program (NAIP) aerial imagery (available at: http://www.atlas.ca.gov/download.html#/casil/imageryBaseMapsLandCover/imagery/naip) collected over the study area in 2005 was used as a reference (already orthorectified) image along with a 10-m digital elevation model (data available from the U.S. Geological Survey: https://viewer.nationalmap.gov/basic/). To achieve a horizontal accuracy of less than 10 m, six iterative stages of coarse alignment were run, followed by three stages of fine alignment. These alignment runs generate and refine ground control points (GCPs) and tie points (TPs) that link the historical imagery to the reference image and match points within overlap areas of adjacent photographs, respectively. In between runs, existing GCPs and TPs were manually examined for accuracy and adjusted if necessary, and new points were added linking clearly identifiable features on the landscape such as rocky outcrops. The final model had 5632 GCPs with root-mean-square error of 7.89 m and 1887 TPs with a root-mean-square error of 1.5 m. Pho-

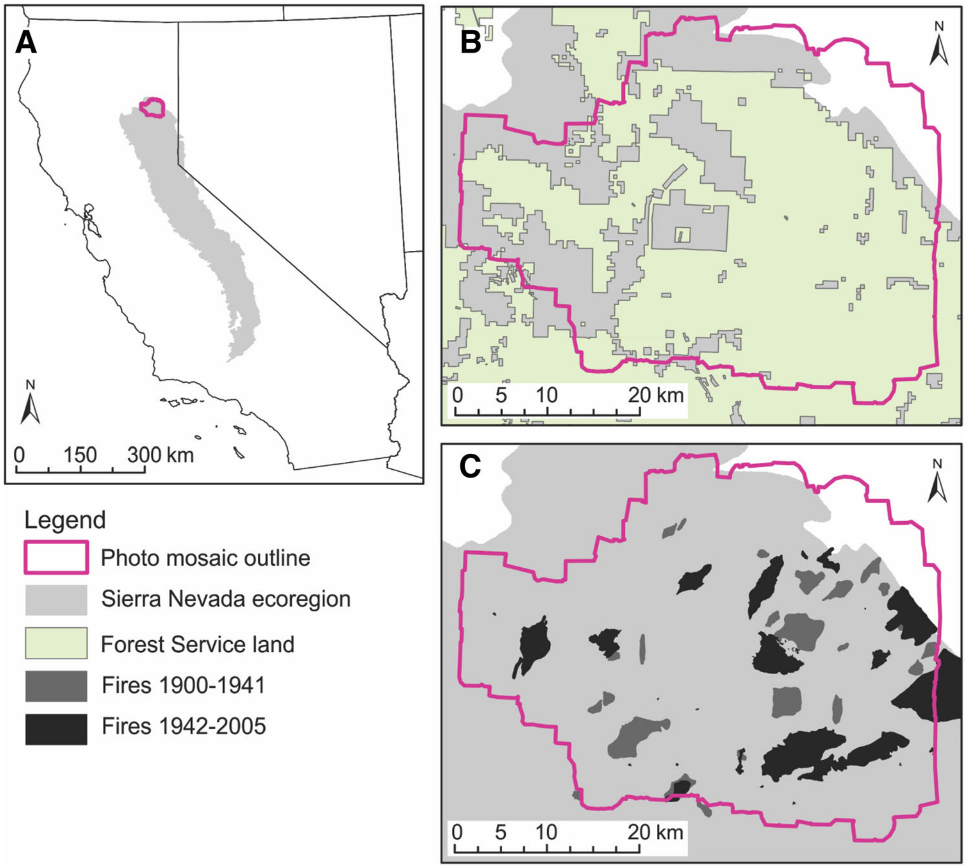

Figure 1. Location of study area within California (**A**), US Forest Service land within the study area (**B**), and extent and location of mapped fires within the study area (**C**).

tograph mosaicking was completed in OrthoEngine (part of the Geomatica software suite) using the neighborhood color balance adjustment and the minimum relative difference method for generating the cut-lines where adjacent photographs were joined. Cut-lines were further adjusted manually to eliminate areas where photograph edges were visible. The resulting photograph mosaic had a resolution of 0.847 m.

A radiometric correction was then applied to the photograph mosaic to compensate for expected differences in illumination due to the effect of aspect and slope on reflectance, using Teillet's C correction (Teillet and others 1982). Although this method does not account for tree shadows that may vary with topographic conditions and canopy complexity (Kane and others 2008), corrections that account for tree shadows work best when canopy cover is greater than 50%, but have high rates of error for forests with lower canopy cover (Gu and Gillespie 1998). Visual inspection of the historical photograph mosaic showed substantial areas with little to no canopy cover and a prevalence of forested areas with the ground clearly visible between trees. We therefore deemed a correction method based on terrain reflectance, which accounts only for the geometry of the land relative to the angle of the sun, rather than canopy reflectance, which also accounts for variation in shadowing due to forest canopy complexity, to be more appropriate for our study area. The solar zenith (angle of the sun relative to directly overhead) and solar azimuth (direction of sun) were calculated based on the time and date for each flight line. However, because a color balance adjustment was used during mosaicking of individual photographs, the average values were used across the landscape rather than using individual photograph values. Average solar zenith was 51.3 (range 44.2–64.4) and average solar azimuth was 190.0 (range 161.2–224.8). Teillet's C correction is calculated as

$$L_n = L\frac{\cos\theta + C}{\cos i + C}, \tag{1}$$

where L_n and L are the corrected and uncorrected illumination values, i is the incidence angle, θ is the

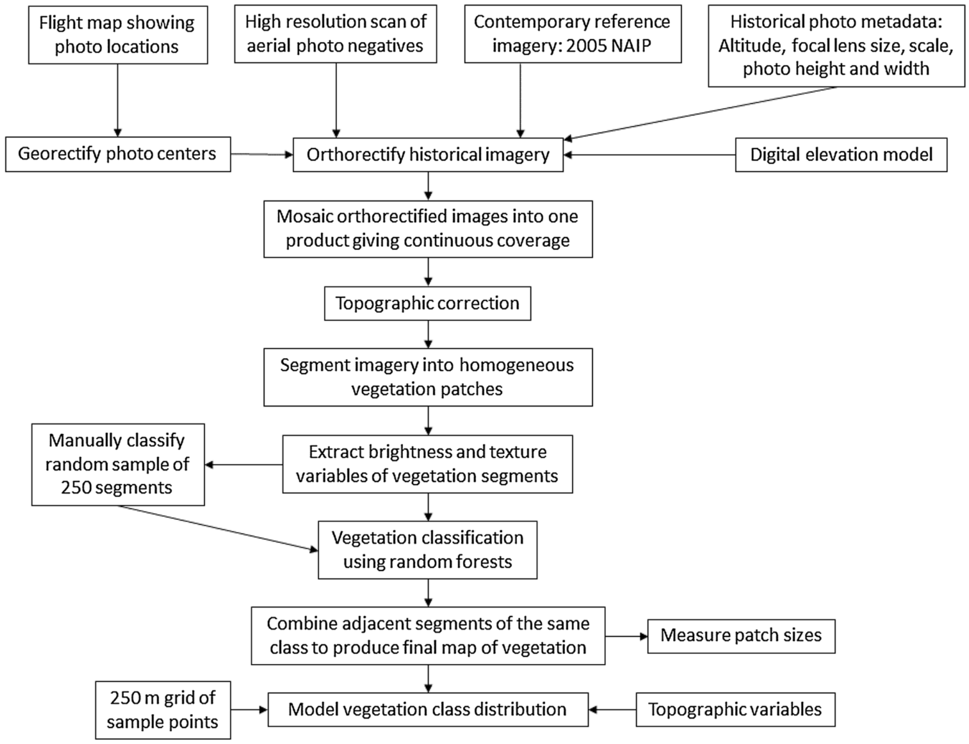

Figure 2. Overview of image processing and analysis steps. NAIP is the National Agriculture Imagery Program.

solar zenith angle, and C is a correction constant unique to the study area (see equations 3 and 4). The incidence angle is calculated as

$$\cos i = \cos\theta\cos\alpha + \sin\theta\sin\alpha\cos\phi, \quad (2)$$

where α is the terrain slope in degrees, and ϕ is the terrain azimuth relative to the sun. C is calculated from the linear relationship derived from the incidence angle, i, and the uncorrected illumination value, L, of pixels within the study area.

$$L = b_0 + b_1 \cos i \quad (3)$$

$$C = \frac{b_0}{b_1} \quad (4)$$

1941 Image Segmentation and Classification

After radiometric correction, the 1941 photograph mosaic was segmented into vegetation patches using the multiresolution segmentation algorithm in eCognition Developer version 9 (Trimble 2016). Multiresolution segmentation consecutively combines adjacent pixels and relies on manual selection of three parameters that affect the size and shape of the resulting segments, or image objects. The scale parameter controls the amount of heterogeneity (for example, variation in pixel shade) allowed within segments and directly affects segment size. The shape parameter weights the influence of spectral versus shape heterogeneity on the scale parameter, with lower values giving greater weight to the spectral imagery (range 0–0.9). The compactness parameter influences the smoothness of the resulting segments, with lower values leading to smoother edges. The compactness parameter modifies the shape parameter, and therefore has little effect when the shape parameter is low. For this study, a scale setting of 175, a shape setting of 0.2, and compactness of 0.5 were used.

After segmentation, the resulting polygons were smoothed in ArcMap, and texture and brightness variables were extracted in eCognition Developer for the vegetation segments. Variables included mean brightness, standard deviation, median, 25th and 75th percentiles, minimum, maximum and skewness of the segment pixels, and texture after Haralick variables based on all directions including GLCM homogeneity, contrast, dissimilarity, entropy, angular second moment, mean, standard deviation, and correlation (Haralick and Shanmugam 1973).

Vegetation classification was based on a set of randomly chosen, manually classified training segments. A training sample of 250 segments was chosen from segments that fell entirely within Forest Service land, thereby excluding urban and agricultural areas on the landscape. Segments for the training sample were selected randomly, using the create random points tool in ArcMap with a minimum distance between points of 500 m. Segments containing these points were then examined visually and manually assigned into four classes of relative forest cover: sparse/open, low, moderate, or dense (Figure 3). This classification was performed over a short period of time by one person to maximize consistency in photointerpretation.

We chose to use four vegetation classes because it would not be possible to assign an accurate and repeatable value of canopy cover to the aerial images. Aerial photographs have increasing distortion approaching the edge of the photograph, relative to the center, particularly with smaller focal lens length (wider angle) (Fensham and Fairfax 2007). This results in trees near the edge of the image appearing larger due to the greater view from the side. As photoscale declines, there may be overestimation of woody cover. For example, Fensham and Fairfax (2007) found that tree crown cover predicted from photographs taken at a 1:80,000 photoscale was 71–91% of the value estimated using photographs taken at a 1:25,000 scale. In addition, in black and white photographs, it is very difficult to distinguish between tree crowns and shadows, and depending on the time of photoacquisition, the size of the shadow will vary making it difficult to compare canopy cover estimates between time points or across an area with multiple acquisitions (Platt and Schoennagel 2009). Although we were unable to quantify canopy cover, we refer to the vegetation classes used as forest cover classes (for example, dense forest cover). We cannot assign a value of canopy cover but the classes are relative to one another. We also were not able to distinguish between vegetation types with very low levels of forest cover (rocky areas, meadows).

After classification of the training sample, the remaining segments in the analysis area were classified into the four forest cover classes with a predictive random forests analysis (RFA) model using brightness and texture variables, along with UTM coordinates of each segment centroid. Segments that fell within water bodies were excluded from the analysis. RFA was performed using the randomForest package in R version 3.03, using a separate model and training dataset for each time period. RFA involves constructing numerous individual regression or classification trees using a randomly selected subset of predictor variables in each tree. Our analysis used 500 individual classification trees and four randomly selected variables per tree. Because class sizes were uneven, a random subset of the training data was selected to build each classification tree, using an equal number of training samples in each class. The classification error rate was assessed using the out of bag error estimates for the RFA model. We also assessed the classification error rate using a second, independent set of manually classified segments (Table S1).

2005 Image Segmentation and Classification

The 2005 NAIP imagery that was used as the reference image during orthorectification of the 1941 aerial photographs was also used to assess vegetation change at the study site. The 2005 NAIP acquisition was made on film at a photoscale of 1:40,000 and had a resolution of 1 m. Note that the photoscale is slightly smaller than the that of the 1941 aerial imagery (1:20,000), which could lead to slight overestimation of canopy cover in 2005 relative to 1941 (Fensham and Fairfax 2007). However, this likely had minimal impact within our coarse classification scheme.

Imagery from 2005 rather than more recent imagery was used because we were interested in vegetation change prior to several large wildfires that occurred in the study area in 2006–2007, which burned 25% of the analysis area. The 2005 image was converted from color to black and white by averaging the red, green, and blue color bands for each pixel across the study area. A radiometric correction similar to that used on the 1941 imagery was not done as the NAIP imagery receives correction prior to distribution (see metadata for details: https://gis.apfo.usda.gov/NAIPMetadata/historic_naip/n_3912002_nw_10_1_20050814.txt). We performed a segmentation on the 2005 reference imagery analogous to that used on the 1941 imagery, using a scale setting of 175, a shape setting of 0.2, and compactness of 0.5.

A classification scheme analogous to that used for the 1941 photograph mosaic was also used for the 2005 image. A separate set of random points was used to select training samples in the historical and reference imagery. The segments in the training sample for the 2005 image were manually classified by the same person as the 1941 imagery to minimize differences in class assignment between time periods. After segments in the training sample were assigned among the four forest cover classes, the remaining vegetation segments from

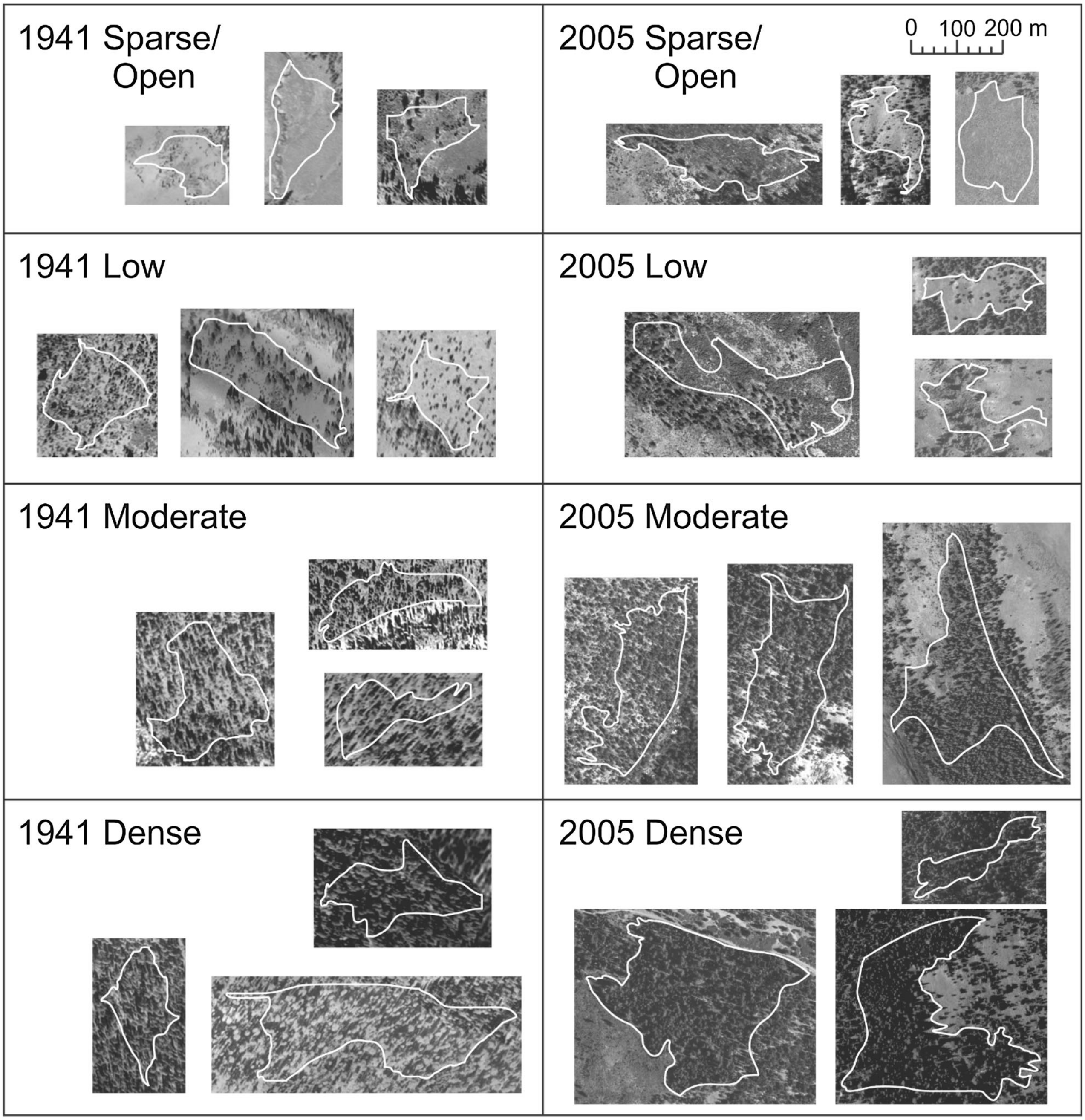

Figure 3. Example training segments for each forest cover class in 1941 and 2005. The white lines are the segment perimeters. All segments are presented at the same scale shown by the scale bar in the upper right corner, and with north oriented up.

the 2005 imagery were classified using the same RFA method as was used for the 1941 vegetation segments. Confidence intervals for estimates of proportional area in each forest cover class were constructed for both classified maps (1941, 2005) using the method described in Olofsson and others (2014). This method uses the error matrix developed by comparing the classification from the training sample (250 segments) to the mapped classes to estimate a standard error for each class and then a 95% confidence interval.

Vegetation Analysis

Final vegetation patches for the two time periods were created by dissolving adjacent vegetation segments that fell into the same forest cover classification in ArcMap, and the total areal extent of

Table 1. Covariates Considered for Inclusion in a Generalized Linear Mixed Model to Predict Occurrence of the Dense Forest Cover Class

Variable	Mean (min–max); or classes	Source
Elevation (m)	1736 (1100–2366)	U.S. Geological Survey, 2013, 1/3 arc-second
Slope (°)	15.4 (0.0–43.0)	Derived from the digital elevation model
Transformed aspect	1.0 (0.0–2.0)	Derived from the digital elevation model, transformed as $1+\cos(45-A)\frac{\pi}{180}$, where A is the aspect in degrees
AET	271.7 (199.57–410.4)	The basin characterization model downscaled climate and hydrology datasets (Flint and others 2013)
Deficit	567.0 (402.4–689.8)	The basin characterization model downscaled climate and hydrology datasets (Flint and others 2013)
TPI	Canyon, ridge, steep slope, gentle slope	Derived from the digital elevation model using CorridorDesigner Toolbox (Majka and others 2007)
TRMI	30.0 (3–52)	Derived from TPI, aspect, slope, and curvature (Parker 1982)

Means and ranges are shown for continuous variables, and classes are shown for categorical variables. TRMI is the topographic relative moisture index, AET is actual evapotranspiration, Deficit is climatic water deficit and TPI is topographic position index. Aspect was transformed using a cosine function, with 45° set to the maximum value of 2.

each class was calculated in both 1941 and 2005. An area-weighted mean (AM) of patch size was calculated for these final patches. The general equation for an area-weighted mean is

$$\mathrm{AM} = \sum_{j=1}^{n} x_{ij} \left(\frac{a_{ij}}{\sum_{j=1}^{n} a_{ij}} \right), \qquad (5)$$

where x_{ij} is the value of patch j within class i for the variable of interest and a_{ij} is the area of patch j within class i. For area-weighted mean patch size $x_{ij} = a_{ij}$. An area-weighted mean gives greater importance to larger patches and better reflects the typical conditions within a given patch type, since a greater proportion of the area will fall within larger patches.

A generalized linear mixed model was used to assess the influence of topographic factors and water balance on dense forest cover in 1941 and 2005 using Proc Glimmix in SAS version 9.3 (Table 1). We chose to focus on dense cover because it was of ecological interest and had the lowest classification error rate. Topographic variables were derived from a 10 m digital elevation model (data available from the US Geological Survey: https://viewer.nationalmap.gov/basic/) in ArcMap. Topographic position index (TPI) was calculated using the CorridorDesigner Toolbox (Majka and others 2007). Topographic relative moisture index was calculated from TPI, aspect, slope, and curvature (Parker 1982). Aspect was transformed using a cosine function, with 45° set to the maximum value of 2 (Table 1). Water balance variables included actual evapotranspiration (AET) and annual climatic water deficit. These variables were obtained as 270 m raster files from the historical version of the California Basin Characterization Model, calculated using 30-year climate normals (1981–2010), updated in 2014 (Flint and others 2013). The water balance variables were resampled from 270 to 10 m using bilinear interpolation to match the scale of the other covariates.

Topographic variables and forest cover class at the two time points were extracted for a 250 m grid of points covering the analysis area, using bilinear interpolation for continuous variables. This grid size was initially chosen to allow for several points within vegetation patches, but the sample size was prohibitively large so only every 30th point was included in the analysis. A spatial power covariance matrix was included in the model to account for spatial autocorrelation between points. Forest cover class was converted to a binary variable representing dense forest cover or non-dense forest cover, including the sparse, low, and moderate forest cover classes. Covariance between variables was assessed using Pearson correlation coefficients, and all variables with $|r| > 0.5$ were removed prior to model selection. TRMI was removed because it was correlated with aspect ($r = 0.62$), and elevation was removed because it was correlated with AET ($r = -0.53$). All other variables had Pearson correlation coefficients with absolute values below 0.5 and were retained. We initially included the remaining set of topographic variables, time period (1941 or 2005), and all interaction terms with time period. Including interaction terms with time period enabled identification of topographic variables that differed in their relationship with dense forest cover in 1941 versus 2005. A stepwise model selection process was used where the least significant variable was removed in each iteration, unless its interaction with time period was significant, until the final model included only significant terms and lower order terms for variables that had significant interactions. To assess model accuracy, we calculated the correct classification rate from the predicted probabilities for the points included in the model selection and for a second, independent set of points from the same 250 m grid.

Results

Classification of forest cover classes using the RFA algorithm had an overall out of bag error rate of 31.6% for the 1941 vegetation segments, and 35.2% for the 2005 vegetation segments. Error rates were similar when comparing class predictions to classes assigned manually for an independent set of vegetation segments (Tables S1 and S2). Misclassifications tended to occur between adjacent (more similar) classes (Tables 2, 3, S1, and S2). For example, dense forest was mainly misclassified as moderate, while moderate was misclassified as both dense and low cover forest. Dense forest had the lowest classification error rate (omission error) in both time points, whereas moderate and low had the highest error rates.

In 1941, the moderate forest cover class was the most abundant across the study area (42%), followed by dense cover (30%, Figure 4). The relative abundance of these two classes was reversed in 2005; dense forest cover was 43% and moderate forest cover was 32% of the study area. There was no overlap between 95% confidence intervals for the dense forest class between time periods, but there was overlap for the moderate class (Figure 4). The proportion of the landscape in low and sparse forest cover showed less change over time, accounting for just 29% of the area in 1941 and 25% of the area in 2005 (Figure 4). Confidence intervals overlapped between time periods for both classes. Although the overall proportions among forest cover classes across the entire landscape did not shift dramatically between 1941 and 2005, their location and spatial pattern changed considerably (Figure 5). The connectivity of vegetation classes, as captured by the area-weighted mean patch size, increased tenfold for the dense forest cover class, from 460 to 4760 ha (Figure 6). Sparse forest cover also increased its patch size, more than doubling from 420 to 960 ha. In contrast, moderate forest became more fragmented, with weighted mean patch size decreasing from 1620 to 650 ha.

Similar to the non-overlapping confidence intervals for the dense cover class, our mixed model results indicated a significant increase in dense forest cover from 1941 to 2005. The final model for predicting the location of dense forest cover on the landscape included slope, time period, and aspect (Table 4). The correct classification rate was 74.6% for the points used in building the model, and 89.5% for a second set of points that were not included in model selection. Aspect was the only variable that had a significant interaction with time

Table 2. Confusion Matrix for Random Forest Classification of Vegetation Segments in 1941 into Four Relative Forest Cover Classes

	Sparse	Low	Moderate	Dense	Total	Omission error
Sparse	17	3	2	0	22	22.7%
Low	4	22	6	0	32	31.3%
Moderate	0	22	86	30	138	37.7%
Dense	0	0	12	46	58	20.7%
Total	21	47	106	76	250	
Commission error	19.0%	53.2%	18.9%	39.5%		31.6%; $\kappa = 0.524$

Rows show the actual (manual) classification, and columns show the predicted classification. The overall classification error rate and the kappa statistic are shown in the bottom right corner.

Table 3. Confusion Matrix for Random Forest Classification of Vegetation Segments in 2005 into Four Relative Forest Cover Classes

	Sparse	Low	Moderate	Dense	Total	Omission error
Sparse	20	8	1	1	30	33.3%
Low	4	13	6	1	24	45.8%
Moderate	1	13	51	23	88	42.0%
Dense	1	2	27	78	108	27.8%
Total	26	36	85	103	250	
Commission error	23.1%	63.9%	40.0%	24.3%		35.2%; κ = 0.472

Rows show the actual (manual) classification, and columns show the predicted classification. The overall classification error rate and the kappa statistic are shown in the bottom right corner.

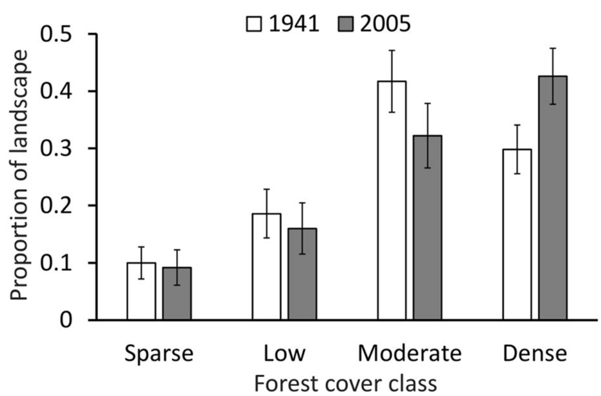

Figure 4. Proportion of Forest Service land within the study area in each forest cover class in 1941 and 2005. Error bars show the 95% confidence intervals, which were derived from the error matrices following the method described by Olofsson and others (2014).

period, indicating a difference in pattern in 1941 and 2005. Across both time periods, transformed aspect had a positive relationship with dense forest cover (that is, denser forest tended to occur at aspect values closer to 45°), but had a stronger effect in 1941 than in 2005 (Table 4, Figure 7). Slope also had a positive relationship with dense forest cover, but the effect was similar in both time periods.

Discussion

The availability of spatially comprehensive aerial photographs, which pre-dated major vegetation changes brought about by timber harvesting, allowed us to robustly capture spatial patterns of historical vegetation in the northern Sierra Nevada. Our analyses comparing historical to contemporary vegetation patterns demonstrated that the extent of dense forest cover increased, replacing moderate forest cover as the dominant class. Concurrent with the increase in extent, the typical patch size of dense forest cover increased substantially, indicating much more homogenous vegetation patterns across the contemporary landscape. Increased forest density and homogenization of vegetation structure at the patch (or stand) scale are commonly noted changes in frequent-fire forests across the Western U.S. (Larson and Churchill 2012; Lydersen and others 2013). The considerable change in landscape vegetation patterns that we demonstrated, however, is relatively novel, since few studies have assessed change at this scale (for example, Hessburg and others 2005).

Although the proportional increase in dense forest cover from 1941 to 2005 was statistically significant, as indicated by both the non-overlapping confidence intervals (Figure 4) and ''time period'' effect from the mixed model analysis (Table 4), the magnitude of change was perhaps lower than expected (30–43%). What may be of more interest than proportional change between vegetation classes is the spatial patterns of change (Levick and Rogers 2011). The tenfold increase in area-weighted mean patch size of the dense cover class (460 ha to 4760 ha, Figure 6) likely reflects a much greater vulnerability to crown fire and insect mortality (Hessburg and others 2005). It is reasonable to assume these increased patch sizes, along with severe fire weather and increased fuel loads, contributed to the uncharacteristically large and severe fires that occurred within our study area after 2005 (Stephens and others 2014). These fires burned with an uncharacteristically large proportion of high-severity fire (51% within the analysis area), with the majority of the high-severity fire occurring in areas classified as dense forest cover in 2005 (Figure 8). Comparing contemporary forest conditions in eastern Washington to those observed in historical aerial imagery, Hessburg and others (2000) also found that forest spatial patterns became more simplified due to an expanded amount

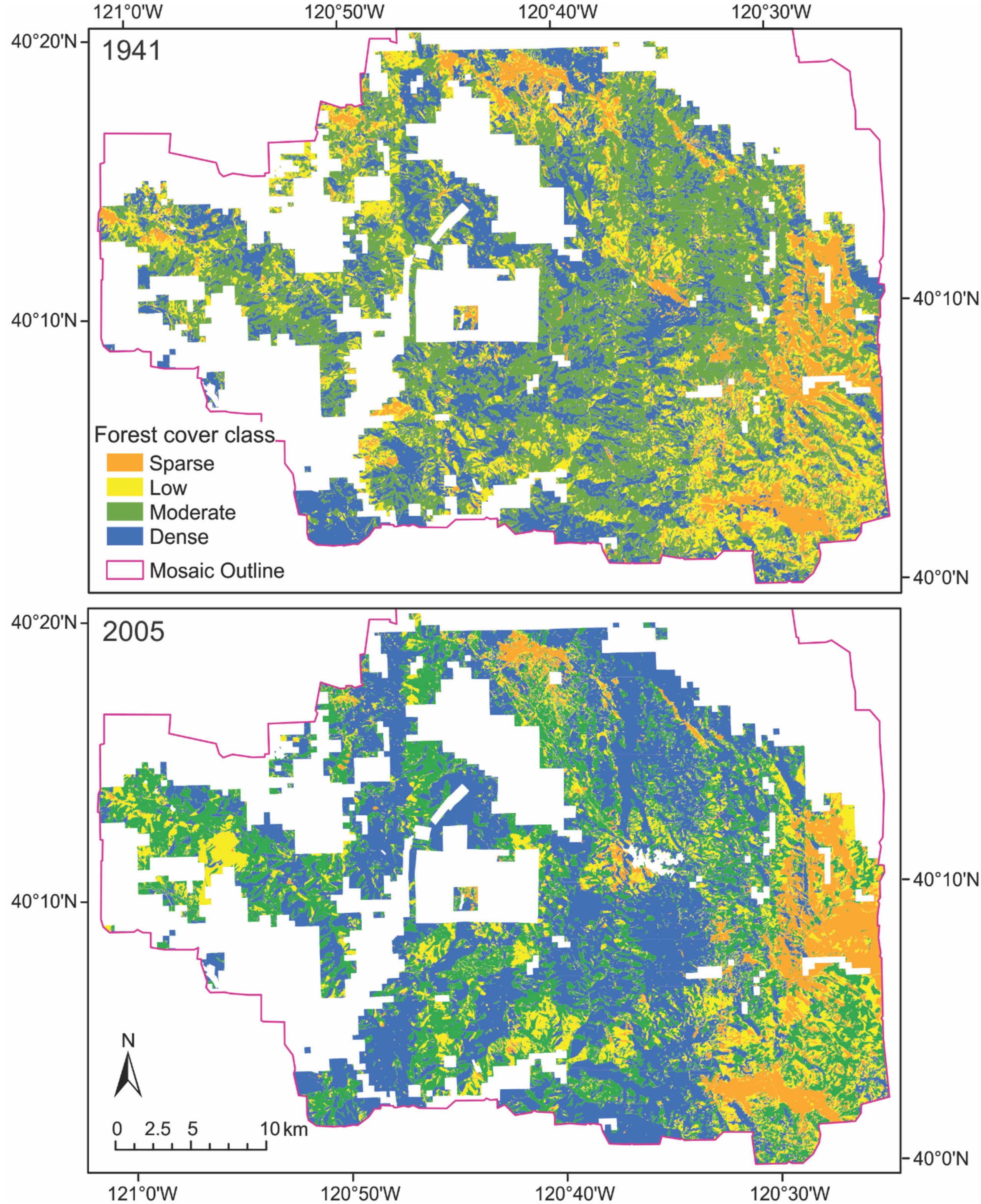

Figure 5. Map showing vegetation classification predicted by random forest analysis across the study area in 1941 and 2005. Non FS lands and water were excluded from the classification.

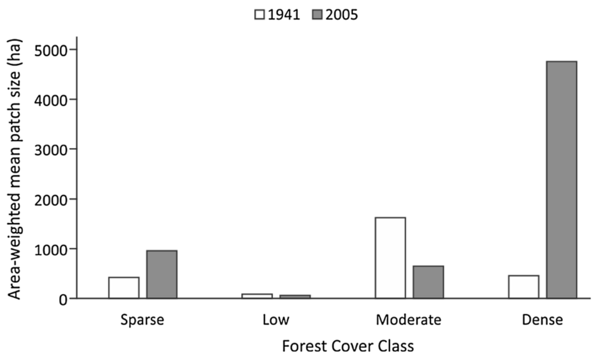

Figure 6. Area-weighted mean patch size of each forest cover class in 1941 and 2005.

and connectivity of intermediate age forest classes, so that dense forest patches had become more vulnerable to stand-replacing fire because they were less isolated than historically.

In addition to altered patch sizes, the topographic patterns of dense forest changed. Dense forest cover was rare on southwesterly aspects (135°–315°) historically, while contemporary dense forest cover was common across a much broader range of aspects (Figure 7). The difference between time periods suggests that infilling of trees occurred on southwesterly slopes, leading to a greater extent of dense forest at drier topographic locations than occurred historically. Analysis of historical aerial photographs of the Colorado Front Range similarly found that tree cover had increased to a greater extent on south-facing slopes and other areas with low forest cover historically (Platt and Schoennagel 2009). The observed increased tree cover on south-facing slopes would also lead to greater fuel accumulation and continuity than occurred historically, leading to greater fire spread potential (Stephens 1998; Lydersen and others 2015). It should be noted that tree density likely also increased on northeasterly slopes, as has been demonstrated with other analyses of forest change over time in relatively productive stands of the Sierra Nevada (for example, Levine and others 2016). A similar association between aspect and forest cover has also been found in Sierra Nevada forests under an active, low-severity fire regime. Lydersen and North (2012) found that contemporary Sierra Nevada forests with a restored fire regime had greater stem density and basal area on northeasterly aspects, and Stephens and others (2015) found that forest classes with greater basal area tended to occur on more northerly aspects in the southern Sierra Nevada in 1911.

Dense forest cover was also found to occur more often on steep slopes, which did not change significantly between time periods. Steep areas may appear to have high density in aerial imagery because the ground distance between trees across a sloped surface is greater than the apparent canopy distance from above due to the slope. This relationship with slope could also be caused by lower-density classes such as meadows, which were included in the sparse/open cover class in our dataset, occurring more often on flatter areas. Finally, even though topographic correction was applied, it is also possible that greater shadowing occurred on steep slopes, leading to a higher misclassification of dense forest on steeper slopes in our analysis.

Although the extent of dense forest cover increased overall, it is likely that some areas decreased in tree cover. The extent of the sparse/open class showed only a marginal decrease (from 10 to 9%), and the low cover class similarly had a very small decrease from 19 to 16% (Figure 4). However, there was a nearly twofold increase in area-weighted mean patch size for the sparse/open forest cover class, from 420 ha to 960 ha (Figure 6). This change in patch size may have been caused by either fire or timber harvesting. Approximately 12,000 ha, or 12% of the analysis area, burned in wildfires between 1941 and 2005. We lack similar detail on the extent and intensity of past timber harvesting over this area, but it is likely that most of the area containing mature trees experienced

Table 4. Solutions for Fixed Effects for a Generalized Linear Mixed Model Estimating the Probability of the Dense Forest Cover Class Occurring Given a Suite of Topographic Variables

Effect	Time period	Estimate	Standard error	*DF*	*t* value	*Pr* > |t|
Intercept		− 1.3291	0.5288	531	− 2.51	0.0122
Slope		0.0307	0.0098	532	3.13	0.0019
Time period	1941	− 1.5925	0.2805	532	− 5.68	< 0.0001
Time period	2005	0	–	–	–	–
Aspect		0.7099	0.1423	532	4.99	< 0.0001
Aspect*time period	1941	0.7255	0.2136	532	3.40	0.0007
Aspect*time period	2005	0	–	–	–	–

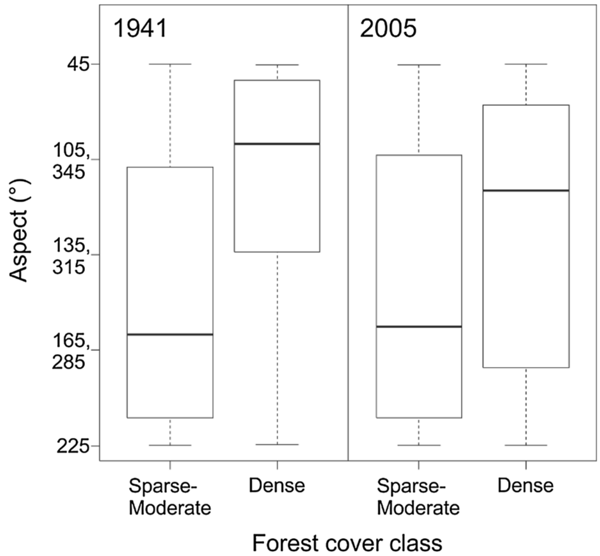

Figure 7. Box and whisker plots comparing aspect between sparse–low–moderate forest cover classes and the dense forest cover class in 1941 and 2005. Dense forest cover was associated with more northeasterly aspects in both time periods, and had a significantly stronger association in 1941 than in 2005 (see Table 4 for statistical analysis output). Aspect was transformed using a cosine function for inclusion in the generalized linear mixed model, with 45° set to the maximum value of 2. It was back-transformed for presentation in this figure. Box and whisker plots depict median (horizontal band), interquartile range (white bar), and range of data within 1.5 interquartile range of the lower and upper quartiles (vertical dashed lines).

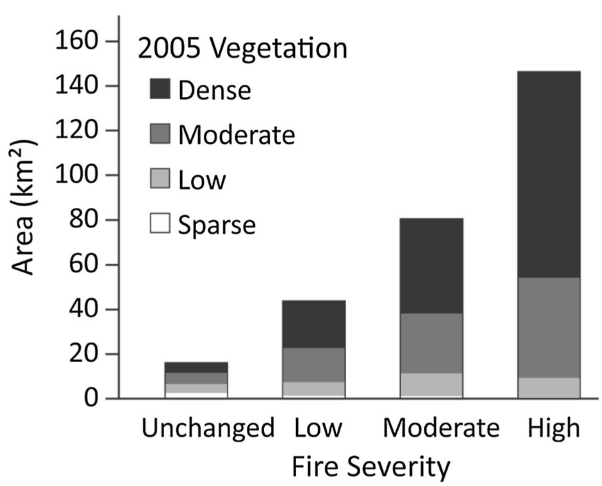

Figure 8. Area in each forest cover class in 2005 among fire severity classes in the area burned by the Moonlight Fire (2007), Antelope Fire (2007) and Boulder Fire (2006) within the analysis area. Fire severity classes are based on the relative differenced normalized burn ratio (Miller and Thode 2007).

selection timber harvests focused on large tree removal (pers. comm., R. Tompkins, Plumas National Forest, 2016). The creation of larger patches in the sparse/open cover class likely compensated for infilling of trees into open patches in other areas (Skinner 1995), so that the shift in proportional cover in this class was minimal. A shift from many small canopy openings to fewer large ones can affect many ecological processes, including tree regeneration patterns, snow pack accumulation, and habitat diversity (White and others 2015; Bales and others 2016; Welch and others 2016).

The amount of relatively dense forest present in the historical landscape is somewhat greater at our study site than has been estimated by other historic datasets for the Sierra Nevada covering a large area. Analyses of forest data from 1911 found that forests with relatively high basal area covered 15% of the study area in the southern Sierra Nevada (Stephens and others 2015), and 10% of the study area in the central Sierra Nevada (Collins and others 2015). This could reflect that a substantial amount of forest infilling had already occurred at our study site by 1941. Forest reconstructions (Scholl and Taylor 2010; Abella and others 2015), historical forest inventory data (Knapp and others 2013; Lydersen and others 2013), and anecdotal observations (Show and Kotok 1924) all demonstrate rapid tree recruitment coinciding with the onset of fire exclusion. Therefore, several decades of tree growth after the onset of fire suppression practices at our study site could have led to greater numbers of small trees and a greater extent of dense cover than was present under an intact frequent-fire regime.

Although the importance of dense forest cover to wildlife in contemporary forests is well understood, how to optimize the spatial configuration of these conditions across frequent-fire landscapes to benefit wildlife is not known (North 2012). It is important to consider the scale at which certain habitat features are important. For example, California spotted owls may be more sensitive to vegetation conditions close to their nest than within their larger territory (Blakesley and others 2005; North and others 2017). However, the presence of any forest with less than 40% canopy cover is negatively correlated with owl territory occupancy (Tempel and others 2016), so the types of vegetation that are interspersed with dense cover may affect habitat value. It is not known what patch size of opening is small enough to avoid having a negative effect on wildlife species that prefer dense cover. Greater connectivity of dense forest is indirectly detrimental since it increases the risk of loss of habitat to wildfire, but this risk can be reduced by implementing a coordinated network of fuels reduction treatments across landscapes (Ager and others 2007; Chiono and others 2017).

There are several limitations to our study that should be considered. One problem, shared by most analyses of historical photography, is a lack of field data to validate the vegetation classification (Eitzel and others 2016). We relied on the out of bag error rate, which uses the misclassification rate of a random subset of the training dataset for each classification tree in the RFA classification. The overall classification accuracies in this study (68.4% for the 1941 imagery and 64.8% for the 2005 imagery) is fairly similar to other studies using automated methods to classify vegetation in historical air photographs. For example, Morgan and Gergel (2013) had accuracy rates ranging from 54 to 64%. Similarly, they also found that misclassifications were more likely between adjacent classes for ordinal classification schemes. However, without historical field data, we were unable to validate the accuracy of the training dataset itself. Errors in the reference dataset can lead to inaccurate estimates of error in the final classification (Foody 2002). Another challenge in using historical air photographs to classify vegetation is that the derived classifications may be lacking in detail. Differentiating between species is difficult due to both the limited range of values in black and white (panchromatic) imagery and differences in tone between different photographs (Morgan and Gergel 2013; Eitzel and others 2015). Because of this, we restricted our classification to four coarse classes of relative forest cover and did not try to differentiate between species or seral stage. Simplifying a continuous variable such as forest cover into discrete categories is also somewhat problematic as it ignores within-category variation (McGarigal and others 2009). Contemporary field data near the timing of the 2005 imagery is likely available in some form, but comparable data around the timing of the 1941 imagery is lacking. This precluded the use of common forest structure metrics such as basal area, stem density, and species composition, which also hindered our ability to relate forest cover classes between time periods. It is likely that the dense forest cover class in 1941 was not equivalent to that in 2005 in terms of its tree size class distribution, species composition, density or basal area, due to both fire exclusion and timber harvesting. This may explain why the overall proportional change in this class was not as large as expected.

Conclusion

Despite the challenges with processing historical aerial photographs and the limitations in what types of information they can provide, the unique information they provide on landscape vegetation patterns make them a valuable source of reference information that can be useful to land managers, as well as for gaining insight into ecosystem dynamics in a less disturbed state. Our analysis showed that the connectivity and size of dense forest patches has increased dramatically since the early 1940s, a trend that likely contributed to the large extent of high-severity fire in the area since 2005. Our study suggests that decreasing the size of dense forest patches, particularly by reducing tree cover on south-facing aspects, could restore historical vegetation patterns and thereby improve forest resilience to wildfire and insect outbreaks.

ACKNOWLEDGEMENTS

We are grateful to the USFS Region 5 Remote Sensing Lab for lending advice and computing resources to help with air photograph processing, particularly Nathan Amboy, Tanya Kohler, Stacey Mikulovsky, and Carlos Ramirez. We thank Nels Johnson at the Pacific Southwest Research Station for help with statistical analysis. We thank Mike Constandy with Westmoreland Research for digitizing all of the historical aerial photographs from the original film stored in the NARA office, College Park, Maryland. Critique and comments from Jeferey Hicke (as subject-matter editor) and two anonymous reviewers improved the clarity and quality of the manuscript. This work was funded by the FY14 Moonlight Fire Restoration Program, project #50 RIRI.

REFERENCES

Abella SR, Chiquoine LP, Sinanian PA. 2015. Forest change over 155 years along biophysical gradients of forest composition, environment, and anthropogenic disturbance. For Ecol Manag 348:196–207.

Ager AA, Finney MA, Kerns BK, Maffei H. 2007. Modeling wildfire risk to northern spotted owl (*Strix occidentalis caurina*) habitat in Central Oregon, USA. For Ecol Manag 246:45–56.

Airey Lauvaux C, Skinner CN, Taylor AH. 2016. High severity fire and mixed conifer forest-chaparral dynamics in the southern Cascade Range, USA. For Ecol Manag 363:74–85.

Bales RC, Zheng Z, Kirchner PB. 2016. Topographic and vegetation effects on snow accumulation in the southern Sierra Nevada: a statistical summary from lidar data. Cryosphere 10:257–269.

Barth MAF, Larson AJ, Lutz JA. 2015. A forest reconstruction model to assess changes to Sierra Nevada mixed-conifer forest during the fire suppression era. For Ecol Manag 354:104–18.

Beaty RM, Taylor AH. 2001. Spatial and temporal variation of fire regimes in a mixed conifer forest landscape, Southern Cascades, California, USA. J Biogeogr 28:955–66.

Beaty RM, Taylor AH. 2008. Fire history and the structure and dynamics of a mixed conifer forest landscape in the northern Sierra Nevada, Lake Tahoe Basin, California, USA. For Ecol Manag 255:707–19.

Blakesley JA, Noon BR, Anderson DR, Boal . 2005. Site occupancy, apparent survival, and reproduction of California spotted owls in relation to forest stand characteristics. J Wildl Manag 69:1554–64.

Boisramé G, Thompson S, Collins B, Stephens S. 2016. Managed wildfire effects on forest resilience and water in the Sierra Nevada. Ecosystems 20:717–32.

Bradford JB, Bell DM. 2017. A window of opportunity for climate-change adaptation: easing tree mortality by reducing forest basal area. Front Ecol Environ 15:11–17.

Brown PM, Wienk CL, Symstad AJ. 2008. Fire and forest history at Mount Rushmore. Ecol Appl 18:1984–99.

Chiono LA, Fry DL, Collins BM, Chatfield AH, Stephens SL. 2017. Landscape-scale fuel treatment and wildfire impacts on carbon stocks and fire hazard in California spotted owl habitat. Ecosphere 8:e01648.

Churchill DJ, Larson AJ, Dahlgreen MC, Franklin JF, Hessburg PF, Lutz JA. 2013. Restoring forest resilience: from reference spatial patterns to silvicultural prescriptions and monitoring. For Ecol Manag 291:442–57.

Clyatt KA, Crotteau JS, Schaedel MS, Wiggins HL, Kelley H, Churchill DJ, Larson AJ. 2016. Historical spatial patterns and contemporary tree mortality in dry mixed-conifer forests. For Ecol Manag 361:23–37.

Collins BM, Kelly M, van Wagtendonk JW, Stephens SL. 2007. Spatial patterns of large natural fires in Sierra Nevada wilderness areas. Landsc Ecol 22:545–57.

Collins BM, Lydersen JM, Everett RG, Fry DL, Stephens SL. 2015. Novel characterization of landscape-level variability in historical vegetation structure. Ecol Appl 25:1167–74.

Dickinson Y. 2014. Landscape restoration of a forest with a historically mixed-severity fire regime: What was the historical landscape pattern of forest and openings? For Ecol Manag 331:264–71.

Eitzel MV, Kelly M, Dronova I, Valachovic Y, Quinn-Davidson L, Solera J, de Valpine P. 2016. Challenges and opportunities in synthesizing historical geospatial data using statistical models. Ecol Inform 31:100–11.

Eitzel MV, Kelly M, Quinn-Davidson LN. 2015. Lessons learned in historical mapping of conifer and oak in the North Coast. Standiford RB, Purcell KL editors. Proceedings of the seventh California oak symposium: managing oak woodlands in a dynamic world. Berkeley, CA: U.S. Department of Agriculture, Forest Service, Pacific Southwest Research Station, pp 521–7.

Fensham R, Fairfax R. 2007. Effect of photoscale, interpreter bias and land type on woody crown-cover estimates from aerial photography. Aust J Bot 55:457–63.

Flint LE, Flint AL, Thorne JH, Boynton R. 2013. Fine-scale hydrologic modeling for regional landscape applications: the California Basin Characterization Model development and performance. Ecol Process 2:25.

Foody GM. 2002. Status of land cover classification accuracy assessment. Remote Sens Environ 80:185–201.

Fulé PZ, Crouse JE, Roccaforte JP, Kalies EL. 2012. Do thinning and/or burning treatments in western USA ponderosa or Jeffrey pine-dominated forests help restore natural fire behavior? For Ecol Manag 269:68–81.

Gu D, Gillespie A. 1998. Topographic normalization of landsat TM images of forest based on subpixel sun–canopy–sensor geometry. Remote Sens Environ 64:166–75.

Hagmann RK, Franklin JF, Johnson KN. 2013. Historical structure and composition of ponderosa pine and mixed-conifer forests in south-central Oregon. For Ecol Manag 304:492–504.

Hagmann RK, Franklin JF, Johnson KN. 2014. Historical conditions in mixed-conifer forests on the eastern slopes of the northern Oregon Cascade Range, USA. For Ecol Manag 330:158–70.

Hagmann RK, Johnson DL, Johnson KN. 2017. Historical and current forest conditions in the range of the Northern Spotted Owl in south central Oregon, USA. For Ecol Manag 389:374–85.

Haralick RM, Shanmugam K. 1973. Textural features for image classification. IEEE Trans Syst Man Cybern 3:610–21.

Hessburg P, Churchill D, Larson A, Haugo R, Miller C, Spies T, North M, Povak N, Belote RT, Singleton P, Gaines W, Keane R, Aplet G, Stephens S, Morgan P, Bisson P, Rieman B, Salter RB, Reeves G. 2015. Restoring fire-prone Inland Pacific landscapes: seven core principles. Landsc Ecol 30:1805–35.

Hessburg PF, Agee JK, Franklin JF. 2005. Dry forests and wildland fires of the inland Northwest USA: contrasting the landscape ecology of the pre-settlement and modem eras. For Ecol Manag 211:117–39.

Hessburg PF, Salter RB, James KM. 2007. Re-examining fire severity relations in pre-management era mixed conifer forests: inferences from landscape patterns of forest structure. Landsc Ecol 22:5–24.

Hessburg PF, Smith BG, Salter RB, Ottmar RD, Alvarado E. 2000. Recent changes (1930s–1990s) in spatial patterns of interior northwest forests, USA. For Ecol Manag 136:53–83.

Johnston JD, Bailey JD, Dunn CJ. 2016. Influence of fire disturbance and biophysical heterogeneity on pre-settlement ponderosa pine and mixed conifer forests. Ecosphere 7:e01581.

Jones GM, Gutiérrez RJ, Tempel DJ, Whitmore SA, Berigan WJ, Peery MZ. 2016. Megafires: an emerging threat to old-forest species. Front Ecol Environ 14:300–6.

Kane VR, Gillespie AR, McGaughey R, Lutz JA, Ceder K, Franklin JF. 2008. Interpretation and topographic compensation of conifer canopy self-shadowing. Remote Sens Environ 112:3820–32.

Kennedy RSH, Wimberly MC. 2009. Historical fire and vegetation dynamics in dry forests of the interior Pacific Northwest, USA, and relationships to Northern Spotted Owl (*Strix occidentalis caurina*) habitat conservation. For Ecol Manag 258:554–66.

Knapp EE, Skinner CN, North MP, Estes BL. 2013. Long-term overstory and understory change following logging and fire exclusion in a Sierra Nevada mixed-conifer forest. For Ecol Manag 310:903–14.

Larson AJ, Churchill D. 2012. Tree spatial patterns in fire-frequent forests of western North America, including mechanisms of pattern formation and implications for designing fuel reduction and restoration treatments. For Ecol Manag 267:74–92.

Larson AJ, Stover KC, Keyes CR. 2012. Effects of restoration thinning on spatial heterogeneity in mixed-conifer forest. Can J For Res 42:1505–17.

Levick SR, Rogers KH. 2011. Context-dependent vegetation dynamics in an African savanna. Landsc Ecol 26:515–28.

Levine CR, Krivak-Tetley F, van Doorn NS, Ansley J-AS, Battles JJ. 2016. Long-term demographic trends in a fire-suppressed mixed-conifer forest. Can J For Res 46:745–52.

Lydersen J, North M. 2012. Topographic variation in structure of mixed-conifer forests under an active-fire regime. Ecosystems 15:1134–46.

Lydersen JM, Collins BM, Brooks ML, Matchett JR, Shive KL, Povak NA, Kane VR, Smith DF. 2017. Evidence of fuels management and fire weather influencing fire severity in an extreme fire event. Ecol Appl 27:2013–30.

Lydersen JM, Collins BM, Knapp EE, Roller GB, Stephens SL. 2015. Relating fuel loads to overstorey structure and composition in a fire-excluded Sierra Nevada mixed conifer forest. Int J Wildland Fire 24:484–94.

Lydersen JM, North MP, Knapp EE, Collins BM. 2013. Quantifying spatial patterns of tree groups and gaps in mixed-conifer forests: Reference conditions and long-term changes following fire suppression and logging. For Ecol Manag 304:370–82.

Majka D, Jenness J, Beier P. 2007. CorridorDesigner: ArcGIS tools for designing and evaluating corridors. Available at http://corridordesign.org.

McGarigal K, Tagil S, Cushman SA. 2009. Surface metrics: an alternative to patch metrics for the quantification of landscape structure. Landsc Ecol 24:433–50.

Miller JD, Thode AE. 2007. Quantifying burn severity in a heterogeneous landscape with a relative version of the delta Normalized Burn Ratio (dNBR). Remote Sens Environ 109:66–80.

Moody TJ, Fites-Kaufman J, Stephens SL. 2006. Fire history and climate influences from forests in the northern Sierra Nevada, USA. Fire Ecol 2:115–41.

Moore MM, Wallace Covington W, Fulé PZ. 1999. Reference conditions and ecological restoration: a southwestern ponderosa pine perspective. Ecol Appl 9:1266–77.

Morgan JL, Gergel SE. 2013. Automated analysis of aerial photographs and potential for historic forest mapping. Can J For Res 43:699–710.

Morgan JL, Gergel SE, Coops NC. 2010. Aerial photography: a rapidly evolving tool for ecological management. Bioscience 60:47–59.

North MP. 2012. Managing Sierra Nevada forests. Albany, CA: USDA Forest Service, Pacific Southwest Research Station. p 184.

North MP, Kane JM, Kane VR, Asner GP, Berigan WJ, Churchill DJ, Conway S, Gutierrez RJ, Jeronimo SMA, Keane J, Koltunov A, Mark T, Moskal LM, Munton TE, Peery MZ, Ramirez CM, Sollmann R, White AM, Whitmore SA. 2017. Cover of tall trees best predicts California spotted owl habitat. For Ecol Manag 405:166–178.

North MP, Stine P, Zielinski W, Stephens S. 2009. An ecosystem management strategy for Sierran mixed-conifer forests. Albany, CA: USDA Forest Service, Pacific Southwest Research Station. p p49.

Olofsson P, Foody GM, Herold M, Stehman SV, Woodcock CE, Wulder MA. 2014. Good practices for estimating area and assessing accuracy of land change. Remote Sens Environ 148:42–57.

Parker AJ. 1982. The Topographic Relative Moisture Index: An approach to soil-moisture assessment in mountain terrain. Phys Geogr 3:160–8.

Platt RV, Schoennagel T. 2009. An object-oriented approach to assessing changes in tree cover in the Colorado Front Range 1938–1999. For Ecol Manag 258:1342–9.

Sánchez Meador AJ, Moore MM, Bakker JD, Parysow PF. 2009. 108 years of change in spatial pattern following selective harvest of a Pinus ponderosa stand in northern Arizona, USA. J Veg Sci 20:79–90.

Scholl AE, Taylor AH. 2010. Fire regimes, forest change, and self-organization in an old-growth mixed-conifer forest, Yosemite National Park, USA. Ecol Appl 20:362–80.

Show SB, Kotok EI. 1924. The role of fire in the California pine forests. Washington, DC: US Dept. of Agriculture.

Skinner CN. 1995. Change in spatial characteristics of forest openings in the Klamath Mountains of northwestern California, USA. Landsc Ecol 10:219–28.

Stephens SL. 1998. Evaluation of the effects of silvicultural and fuels treatments on potential fire behaviour in Sierra Nevada mixed-conifer forests. For Ecol Manag 105:21–35.

Stephens SL, Bigelow SW, Burnett RD, Collins BM, Gallagher CV, Keane J, Kelt DA, North MP, Roberts LJ, Stine PA, Van Vuren DH. 2014. California spotted owl, songbird, and small mammal responses to landscape fuel treatments. Bioscience 64:893–906.

Stephens SL, Lydersen JM, Collins BM, Fry DL, Meyer MD. 2015. Historical and current landscape-scale ponderosa pine and mixed conifer forest structure in the Southern Sierra Nevada. Ecosphere 6:art79.

Stephens SL, Miller JD, Collins BM, North MP, Keane JJ, Roberts SL. 2016. Wildfire impacts on California spotted owl nesting habitat in the Sierra Nevada. Ecosphere 7:e01478.

Teillet P, Guindon B, Goodenough D. 1982. On the slope-aspect correction of multispectral scanner data. Can J Remote Sens 8:84–106.

Tempel DJ, Gutiérrez RJ, Battles JJ, Fry DL, Su Y, Guo Q, Reetz MJ, Whitmore SA, Jones GM, Collins BM, Stephens SL, Kelly M, Berigan WJ, Peery MZ. 2015. Evaluating short- and long-term impacts of fuels treatments and simulated wildfire on an old-forest species. Ecosphere 6:art261.

Tempel DJ, Keane JJ, Gutiérrez RJ, Wolfe JD, Jones GM, Koltunov A, Ramirez CM, Berigan WJ, Gallagher CV, Munton TE, Shaklee PA, Whitmore SA, Peery MZ. 2016. Meta-analysis of California spotted owl (*Strix occidentalis occidentalis*) territory occupancy in the Sierra Nevada: habitat associations and their implications for forest management. Condor 118:747–65.

Tingley MW, Ruiz-Gutiérrez V, Wilkerson RL, Howell CA, Siegel RB. 2016. Pyrodiversity promotes avian diversity over the decade following forest fire. Proc R Soc B 283:20161703.

Van de Water KM, Safford HD. 2011. A summary of fire frequency estimates for California vegetation before Euro-American settlement. Fire Ecol 7:26–58.

Welch KR, Safford HD, Young TP. 2016. Predicting conifer establishment post wildfire in mixed conifer forests of the North American Mediterranean-climate zone. Ecosphere 7:e01609.

White AM, Manley PN, Tarbill GL, Richardson TW, Russell RE, Safford HD, Dobrowski SZ. 2015. Avian community responses to post-fire forest structure: implications for fire management in mixed conifer forests. Anim Conserv 19:256–64.

Young DJN, Stevens JT, Earles JM, Moore J, Ellis A, Jirka AL, Latimer AM. 2017. Long-term climate and competition explain forest mortality patterns under extreme drought. Ecol Lett 20:78–86.